

The temperature dependence of mobility and photocurrent on *p*-type photoconductive CuInSe₂ layers and their application in *n*-CdS/*p*-CuInSe₂ solar-cells

J. W. Jeong^a, J. J. Bang^a, K. J. Hong^{a,*}, T. S. Jeong^b and C. J. Youn^b

^aDepartment of Physics, Chosun University, Gwangju 501-759, South Korea

^bSemiconductor Physics Research Center (SPRC), School of Semiconductor and Chemical Engineering, Chonbuk National University, Jeonju 561-756, South Korea

Copper indium diselenide (CIS) layers, which are now showing promise as solar-cell materials, were successfully grown on GaAs (100) substrates using the hot wall epitaxy (HWE) method. The photoconductive CIS layers were grown along the <112> direction having a beneficial gain for solar energy conversion. From the Hall effect measurements, the mobility tended to decrease as a function of $T^{-3/2}$ in the high temperature range ($T > 130$ K), and increase as a function of $T^{3/2}$ in the a low temperature range ($T < 50$ K). Also, from the photocurrent (PC) measurements, three peaks, A, B, and C, corresponded to the intrinsic transition from the valence band states of $\Gamma_7(A)$, $\Gamma_6(B)$, and $\Gamma_7(C)$ to the conduction band state of Γ_6 , respectively. The temperature dependence of the optical band gap obtained by the PC measurements could be expressed by using the empirical equation $E_g(T) = E_g(0) - (8.57 \times 10^{-4})T^2/(T + 129)$. By conducting solar cell fabrications, a 14.3% efficiency for *n*-CdS/*p*-CIS heterojunction solar-cells was achieved. This achievement suggests that the improved quality of the absorber layer, grown using the HWE method, contributes to the high performance of CIS solar cells.

Key words: Copper indium diselenide (CIS), mobility, Photocurrent, *n*-CdS/*p*-CIS heterojunction solar-cell, Solar energy conversion efficiency.

Introduction

In order to be good photovoltaic (PV) materials, they need to have strong light absorption, low cost, stability (as a function of both time and illumination conditions), high abundance of source materials, and be environmentally-friendly. Copper indium diselenide (CuInSe₂, CIS), which crystallizes to a chalcopyrite structure, has received considerable attention in recent years because of its applications in PV devices [1-3]. Thus, a photocurrent (PC) investigation of CIS had been made for the applications of photodetection and radiation measurement [4]. Although photoconductivity is a complex process involving thermal and hot carrier relaxation processes, charge carrier statistics, effects of electrodes, and several mechanisms of recombination, it is also important to investigate the conductivity changes in photoconductive CIS caused by incident radiation. In PC measurements, the absorbed photons with a higher energy than the band-gap energy, create electron and hole carriers. If an external electric field is applied, the electrons and holes move in opposite directions, and produce PC signals. These carriers instantly flow out through the electrodes. Thereby, the PC peak obtained corresponds to the direct band-gap energy. Moreover,

the electronic transitions from the levels of the valence band to the levels of the conduction band are restricted by a selection rule based on the symmetry in the Brillouin zone [5]. Consequently, the photoresponse measurement offers us valuable information about the band-gap energies in the higher energy stages.

On the other hand, CIS for solar cells are: (1) a capable material for solar cells with high efficiency in spite of a thickness of 1 ~ 2 μm , (2) a cheaper material in comparison to crystalline Si (sharing about 90% of the Si solar-cell market), (3) and a material having better electro-optical stability for long periods time. Moreover, it is one of the most environmental-friendly materials for Cd-free buffer layers because of its high absorbance of radiation in the ultraviolet (UV) visible range [6]. The band gap of CIS is about 1 eV, which is capable of absorbing all light wavelengths. However, the open-circuit voltage (V_{oc}) on CIS solar cells of a *p-n* heterojunction structure is of a comparatively low value below 0.5 V. Currently, it has been reported that CIS-based solar cells achieved a high conversion efficiency of 19.2% [7]. Despite these technological progresses, many of the fundamental properties of CIS are still not fully understood.

In this paper, the CIS layers, which could be used for absorbance in solar cells, were grown on a GaAs substrate by a hot wall epitaxy (HWE) method. The fundamental properties were investigated through X-ray diffraction (XRD), low-temperature photoluminescence

*Corresponding author:
Tel : +82-62-230-6637
Fax: +82-62-234-4326
E-mail: kjhong@chosun.ac.kr

(PL), and the Hall effect. By measuring PC spectra at different temperatures, we discussed the valence band splitting and the temperature dependence of the band-gap energy on the CIS layers. Furthermore, CIS-based solar cells were investigated.

Experimental

Prior to layer growth, polycrystalline CIS was synthesized. The starting materials were 6N purity shot-types of Cu, In, and Se. After the materials were weighed to the mole fraction of each element, they were sealed in a quartz tube to maintain a vacuum atmosphere. Then, they were synthesized in a horizontal polycrystalline-synthesis furnace. To grow the CIS layers, the ingot of CIS polycrystalline was used as a HWE source. The CIS layers were grown on semi-insulating (100) GaAs by the HWE method using the grown CIS ingot as a source material. Figure 1 presents a diagram of the HWE apparatus used for the CIS growth and solar-cell sample. In this experiment, the CIS layer was grown by using furnace (a) as shown in Fig. 1. Prior to growing the CIS layers, the GaAs substrate was cleaned ultrasonically for 1 minute in successive baths of trichloroethylene, acetone, methanol, and 2-propanol, and then etched for 1 minute in a solution of H₂SO₄ : H₂O₂ : H₂O (5 : 1 : 1). The substrate was degreased in organic solvents and rinsed with deionized water (18.2 MW). After the substrate was dried off, it was immediately loaded onto the substrate holder in Fig. 1 and was annealed at 580 °C for 20 minutes to remove the residual oxide on the surface of the substrate. To obtain optimum growth conditions, grown CIS layers were estimated through low-temperature PL and XRD measurements. With a source temperature of 620 °C obtained through experimental repetition, the most suitable substrate temperature for growth turned out to be 410 °C. Thus, the grown CIS layers were obtained with a thickness of 2.7 μm and a growth rate of 0.9 μm/h. Also, the growth direction of

the CIS layer grown on the GaAs (100) was found to be the <112>. Thus, the observation of only one peak, CIS (112), indicates that the CIS layer was epitaxially grown along the <112> direction on the GaAs (100) substrate. This orientation has been suggested as beneficial for a CIS layer fabricated for solar energy conversion [8]. Detailed growth procedures have been published elsewhere [9].

The Hall effect experiments were carried out using the Van der Pauw method. In order to record the PC measurements, two Au electrodes with a coplanar geometry on the CIS layer were fabricated by an e-beam evaporator, and the Ohmic contact of the electrodes was confirmed by a current-voltage measurement. After the electrodes were connected to a wire, the sample was mounted on the holder of a low-temperature cryostat. The PC spectrum measurements were taken while monochromatic light emitted from a halogen lamp passed through a chopper to illuminate the sample.

Also, the CdS/CIS bilayers for the solar-cell specimen were grown in situ using HWE, as shown in Fig. 1. The substrate of a Pyrex glass, which was sprayed with indium tin oxide (ITO), was moved successively to the top from the furnace (a) to (b). The source materials 1 and 2, as shown in Fig. 1, were a polycrystalline CIS ingot and CdS powder (Rare Metallic, 6N), respectively. After the CIS layer on the ITO glass was grown in furnace (a), the CIS/ITO layer was immediately moved to furnace (b). Then, the CdS/CIS/ITO layer was grown using heating source 2. Also, the solar-cell measurements were conducted by illuminating with a tungsten halogen lamp at 80 mW/cm².

Results and Discussion

Temperature dependence of mobility and photocurrent

Figure 2 shows the temperature dependence of the Hall mobility. The mobility tended to increase during the lowering of the temperature to 100 K, after which it decreased. At the apex at 100 K, it showed the largest value of 998 cm²/V s. As shown in Fig. 2, the mobility

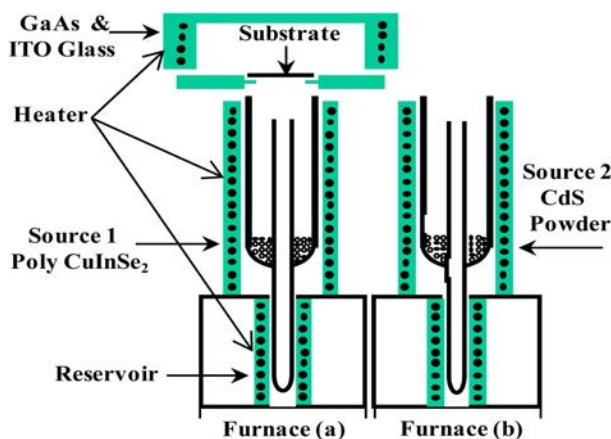


Fig. 1. Diagram of the HWE apparatus used for the CIS growth (a) and solar-cell specimen (b)

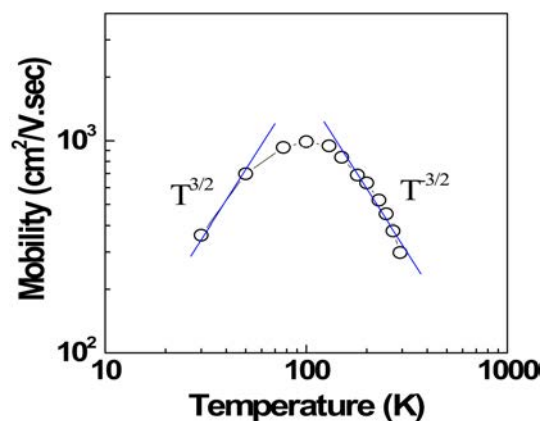


Fig. 2. Temperature dependence of the Hall mobility obtained from the Hall effect measurements

in the high temperature range ($T > 130$ K) tended to decrease as a function of $T^{-3/2}$ by increasing the temperature, and increase as a function of $T^{3/2}$ in the low-temperature range ($T < 50$ K). This indicates that scattering in the high-temperature range is mainly due to the acoustic mode of lattice vibrations through a deformation potential and that scattering at low-temperature range is most pronounced due to the impurity effect [10]. From the result of the Hall coefficient values, the grown CIS layer was confirmed to be *p*-type. The grown sample was always *p*-type presumably due to slight stoichiometric deviations originating from an excess of copper vacancies (V_{Cu}), which is a shallow acceptor. Thus, the shallow-acceptor value was determined to be 61 meV from the relation between the reciprocal temperature and the carrier concentration. This value is nearly equal to the shallow acceptor of 60 meV due to the low or no Cu-excess [11].

Figure 3 shows the PC spectra of a *p*-type photoconductive CIS layer at temperatures ranging from 10 to 293 K. Three peaks appeared in each PC spectrum for a given temperature, as shown in Fig. 3. These peak positions at 293 K were located at 1224.9 (1.0121 eV), 1217.8 (1.0180 eV), and 993.4 nm (1.2481 eV). These PC peaks represent the intrinsic transitions caused by the band-to-band transitions [12, 13]. The electrons excited from the valence band to the conduction band by the absorbed photons flow immediately through the electrodes. Then, only the PC peaks corresponding to the band gap are detected. According to the selection rule, the peak at 1.0121 eV, peak "A", is ascribed to the electronic transition from the $\Gamma_7(A)$ valence band to the Γ_6 conduction band. The peak at 1.0180 eV, peak "B", is associated with the electronic transition from the $\Gamma_6(B)$ valence band to the Γ_6 conduction band, and the peak at 1.2481 eV, peak "C", is ascribed to the electronic transition from the $\Gamma_7(C)$ valence band to the

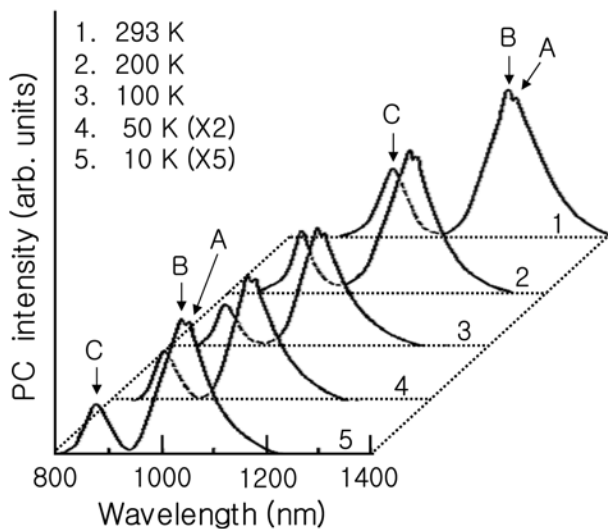


Fig. 3. PC spectra of a *p*-type photoconductive CIS layer at temperatures ranging from 10 to 293 K.

Γ_6 conduction band. In spite of the decrease of the measurement temperature, these three peaks were continuously observed until the lowest temperature. At 10 K, it is suggested that the three peaks at 1047.2 (1.1839 eV), 1041.4 (1.1898 eV), and 873.2 nm (1.4199 eV) correspond to the peaks A, B, and C, respectively.

Figure 4 displays the variation of the band-gap energy as a function of temperature on the CIS layer obtained from PC measurement. A PC measurement is one of the useful methods for the band-gap determination of the CIS layer. In fact, the absorption experiment has been known to be inaccurate for obtaining the band gap energy because of the difficulty in defining the position of the absorption edge, but the PC measurement can directly give the energy corresponding to the band gap by measuring the PC peak position. The temperature dependence of the optical band-gap energy in our experiment is well fitted numerically by the following formula [14, 15]:

$$E_g(T) = E_g(0) - \alpha T^2 / (T + \beta) \quad (1)$$

where α is a constant and is approximately the Debye temperature. Also, $E_g(0)$ is the band-gap energy at 0 K, which is estimated to be 1.187 eV. When α and β are taken to be 8.57×10^{-4} eV/K and 129 K, respectively, the curve plotted by Eq. 1 closely fits the experimental values.

Solar cell properties

Figure 5 presents the spectral response of the *n*-CdS/*p*-CIS bilayer. This spectral response was determined while monochromatic light illuminated on the sample. As shown in Fig. 5, the spectrum is widely distributed from 300 to 1400 nm. A spectral response at the wavelength of 525.4 nm was sensitively detected, and this position corresponds to the band gap of CdS. This

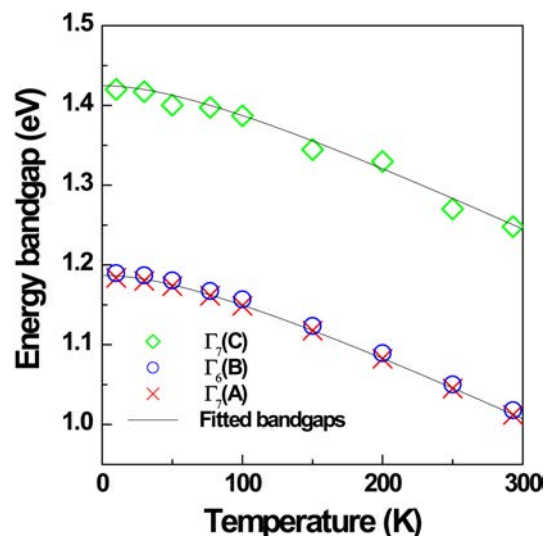


Fig. 4. Variation of the band-gap energy as a function of temperature on the CIS layer obtained from PC measurements.

spectral response was maintained until the wavelength of 1223.4 nm, after which the intensity decreased. This suggests that the wavelength of 1223.4 nm is related to the band gap of the CIS. Therefore, this means that the photon which passed through the CdS layer is well absorbed in the CIS layer.

CIS-based solar cells were investigated. Figure 6 shows the dark and illuminated current density-voltage (*J*-*V*) characteristics of *n*-CdS/*p*-CIS heterojunction solar cells. Also, the sub figure in Fig. 6 shows a schematic diagram of the *n*-CdS/*p*-CIS heterojunction. It is fabricated to a *p*-*n* junction between the *p*-CIS layer as the absorber material and the *n*-CdS layer. In the dark, the device follows the well-known rectifying *J*-*V* characteristic of the simple *p*-*n* diode. But, under illumination, it is considered to be at the current

density (*J*_{light}) generated by the photon absorption. Therefore, the ideal *J*-*V* characteristics for *p*-*n* junction solar cells are given as [10]:

$$J = J_{\text{dark}} - J_{\text{light}} = J_0[\exp(qV/kT) - 1] - J_{\text{light}}, \quad (2)$$

where *J* is the current density flowing through the solar cell, *J*₀ the saturation current, *q* the electrical charge, *V* the applied voltage, *k* the Boltzmann constant, and *T* the temperature of the solar cell. Therefore, the maximum power (*P*_{max}) can be extracted out from the area of the indicated rectangle (*P*_{max} = *V*_{max} × *J*_{light}). The fill factor, FF, is given as FF = (*V*_{max} × *J*_{light})/(*V*_{oc} × *J*_{sc}), where *J*_{sc} is the short-circuit current-density. The power conversion efficiency, η, of a solar cell is given as:

$$\eta = (FF \times V_{\text{oc}} \times J_{\text{sc}}) / P \quad (3)$$

where *P* is the illumination power. The *V*_{oc}, *J*_{sc}, and FF were obtained to be 0.51 V, 29.3 mA/cm², and 0.76, respectively. Thus, the on *n*-CdS/*p*-CIS heterojunction solar cells were estimated to be 14.3% efficient from Eq. 3. The solar-cell parameters obtained from the *J*-*V* characteristic are given in Table 1. As Table 1 shows, an efficiency of 14.3% which is closely equal to the 14.8% obtained by a solar cell with a *n*-ZnO/*n*-CdS/*p*-CIS structure deposited on a soda-line glass substrate [16]. It is comparatively more efficient in spite of not having another window, such as ZnO. This cause is related to the absorber-material improvement of CIS layer. Our absorber material of CIS has a stoichiometric formation as mentioned above. So, it has low defect density. Consequently, it suggests that the improved quality of the absorber layer grown using the HWE method contributed to the improved performance of CIS solar cells.

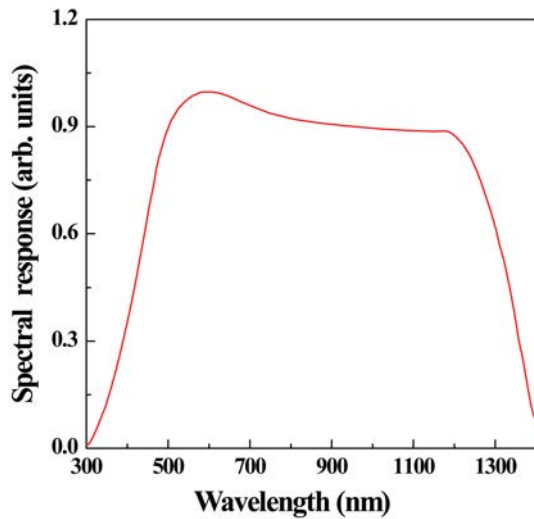


Fig. 5. Spectral response of the *n*-CdS/*p*-CIS bilayer.

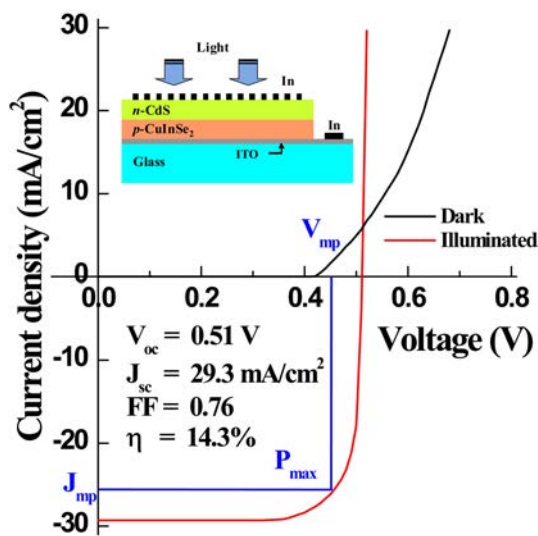


Fig. 6. Dark and illuminated current density-voltage characteristics of *n*-CdS/*p*-CIS heterojunction solar cells (Here, the subfigure shows a diagram of the *n*-CdS/*p*-CIS junction. Also, *J*_{mp} and *V*_{mp} are the current density and voltage values at the maximum power point *P*_{max}, respectively.)

Conclusions

Photoconductive CIS layers were successfully grown on GaAs(100) substrates through the HWE method. Under optimized condition, the CIS layer was

Table 1. Comparison of the *J*-*V* parameters on the *n*-CdS/*p*-CIS solar-cells.

Cell	<i>V</i> _{oc} (V)	<i>J</i> _{sc} (mA/cm ²)	FF	Efficiency (%)	Reference
ZnO/CdO/CIS layer	0.513	40.4	0.716	14.8	[16]
CdS/CIS layer	0.36	32.8	0.58	6.9	[17]
ZnO/CdS/CIS multilayers	0.417	37.9	0.606	9.59	[18]
ZnO/CdO/CIS layer	0.697	21.5	0.69	10.2	[19]
CdS/CIS layer	0.51	29.3	0.76	14.3	This work

confirmed to be an epitaxially grown layer along the $\langle 112 \rangle$ direction having a beneficial gain for solar energy conversion. From the Hall effect measurements, the mobility was determined to be $129 \text{ cm}^2/\text{V} \cdot \text{s}$ at 293 K. In the high temperature range ($T > 130 \text{ K}$), it tended to decrease as a function of $T^{-3/2}$ by increasing the temperature, and increase as a function of $T^{3/2}$ in the low-temperature range ($T < 50 \text{ K}$). Also, in the PC experiments, three peaks due to band-to-band transitions were observed in the total temperature range. From that, the A, B, and C peaks obtained were associated with the intrinsic transitions from the valence band state of $\Gamma_7(\text{A})$, $\Gamma_6(\text{B})$, and $\Gamma_7(\text{C})$ to the conduction band state of Γ_6 , respectively. The temperature dependence of the optical band gap could be well expressed by using Varshni's formula: $E_g(T) = E_g(0) - \alpha T^2/(T + \beta)$, where α and β were $8.57 \times 10^{-4} \text{ eV/K}$ and 129 K, respectively. Furthermore, the CdS/CIS bilayers for the solar-cell fabrication were grown in situ on ITO Pyrex glass using the HWE method first. The photoresponse spectrum of the bilayer was widely distributed from 300 to 1400 nm. Under illumination, the V_{oc} , J_{sc} , and FF were obtained to be 0.51 V, 29.3 mA/cm^2 , and 0.76, respectively. Thus, the on n -CdS/ p -CIS heterojunction solar cells was found to be 14.3% efficient having a comparatively higher efficiency. This is related to the quality improvement of the CIS layer. Consequently, it suggests that the improved quality of the absorber layer grown using the HWE method contributed to the higher performance of the CIS solar cells.

Acknowledgments

This study was supported by research funds from Chosun University, 2011.

References

1. J.L. Shay, J.H. Wernick, Ternary Chalcopyrite Semiconductors: Growth, Electronic Properties, and Applications, Pergamon, Oxford 2 (1975).
2. A. de Kergommeaux, A. Fiore, N. Bruyant, F. Chandezon, P. Reiss, A. Pron, R. de Bettignies, J. Faure-Vincent Sol. Energy Mater Sol. Cells 95 (2011) S39-S43.
3. K.H. Lam, J. Durisch, W. Close, Solar Energy 77 (2004) 121-124.
4. N.V. Joshi, Photoconductivity: Art, Science, and Technology, Marcel Dekker, New York (1990).
5. K.L. Greenaway, G. Harbeke, Optical Properties and Band Structure of Semiconductors, Pergamon, Oxford (1968).
6. M. Yamaguchi, J. Appl. Phys. 78(1995) 1476-1481.
7. K. Ramanathan, M.A. Contreras, C.L. Perkins, S. Asher, F.S. Hasoon, J. Keane, D. Young, M. Romero, W. Metzger, R. Noufi, J. Ward, A. Duda, Prog. Photovolt Res. Appl. 11(2003) 225-229.
8. M.D. Kannan, R. Balasundaraprabhu, S. Jayakumar, P. Ramanathaswamy, Solar Energy Mater. Sol. Cells 81 (2004) 379-383.
9. S.H. You, K.J. Hong, B.J. Lee., J.J. Bang, T.S. Jeong., C.J. Youn, J. Korean Phys. Soc. 50(2007) 1784-1789.
10. S.M. Sze, Semiconductor Devices Physics and Technology, Wiley, New York (1985).
11. S. Siebentritt, N. Rega, A. Zajogin, M. Lux-Steiner, Phys. Stat. Sol. (c)9 (2004) 2304-2309
12. S.H. You, K.J. Hong, T.S. Jeong, C.J. Youn, J.S. Park, D.C. Shin, J.D. Moon, J. Cryst. Growth 256 (2003) 116-120.
13. C.C. Klick, Phys. Rev. 89 (1953) 274-279.
14. Y.P. Varshni, Physica. 34 (1967) 149-154.
15. K.J. Hong, T.S. Jeong, C.J. Yoon, Y.J. Shin, J. Cryst. Growth 218 (2000) 19-24.
16. L. Stolt, J. Hedstrom, J. Kessler, M. Ruckh, K. Velthaus, H.W. Schock, J. Appl. Phys. Lett. 62 (1993) 597-601.
17. Y. Okano, T. Nakada, A. Kunioka, Sol. Energy Mater Sol. Cells 50 (1998) 105-109.
18. D.Y. Lee, J.H. Yun, K.H. Yoon, B.T. Ahn, Thin Solid Films 410 (2002) 171-175.
19. R. Scheer, T. Walter, H.W. Schock, M.L. Fearheiley, H. Leweren, J. Appl. Phys. Lett. 63 (1993) 3294-3298.